X-632-64-243

TM X-55094

N64 33566

(ACCESSION NUMBER) 53 (PAGES) TMX-55094 (NASA CR OR TMX OR AD NUMBER)

(THRU) 1 (CODE) 08 (CATEGORY)

FACILITY FORM 602

# A VERTICAL TEST RANGE FOR ANTENNA RADIATION MEASUREMENTS

BY

JOHN STECKEL

AND

WILLIAM KORVIN

OTS PRICE

XEROX $ 3.00 FS

MICROFILM $ 0.50 MF

JULY 1964

GODDARD SPACE FLIGHT CENTER

GREENBELT, MD.

# A VERTICAL TEST RANGE FOR ANTENNA RADIATION MEASUREMENTS

By

John Steckel and William Korvin

July 1964

Spacecraft Technology Division
Spacecraft Electronics Branch

Goddard Space Flight Center
Greenbelt, Maryland

ABSTRACT



In order to facilitate the measuring of satellite antenna radiation patterns under a controlled RF environment the concept of a "Vertical RF Test Range" was devised. The vertical test range configuration is shown in Figure 1.

Of primary importance was the test range's capability to adequately absorb and/or suppress undesirable electromagnetic energy as low as 125 Mc which would normally be reflected from the chamber walls and floor. The satellite antennas of concern are of the broad-pattern, near-omnidirectional type (i. e., dipole, turnstile, etc.).

The preliminary study, investigation, and 1/9-scale chamber model measurements indicated that a feasible reflection coefficient level of the order of 20 db to 25 db can be expected in an electrically small chamber of approximately $2\lambda \times 2\lambda \times 1\lambda$ in size. Subsequent full-scale measurements in the completed chamber have verified these reflection coefficient levels.

At higher frequencies of operation it was anticipated (and also indicated by 1/9-scale chamber model measurements) that the reflected energy level would be lower. The dominant controlling factor at higher frequencies is the structural weather protective radome. At the lower frequency the radome appears as a very thin wall (approximately $0.05\lambda$ thick). But as the frequency is increased, the presence of the radome becomes increasingly significant.

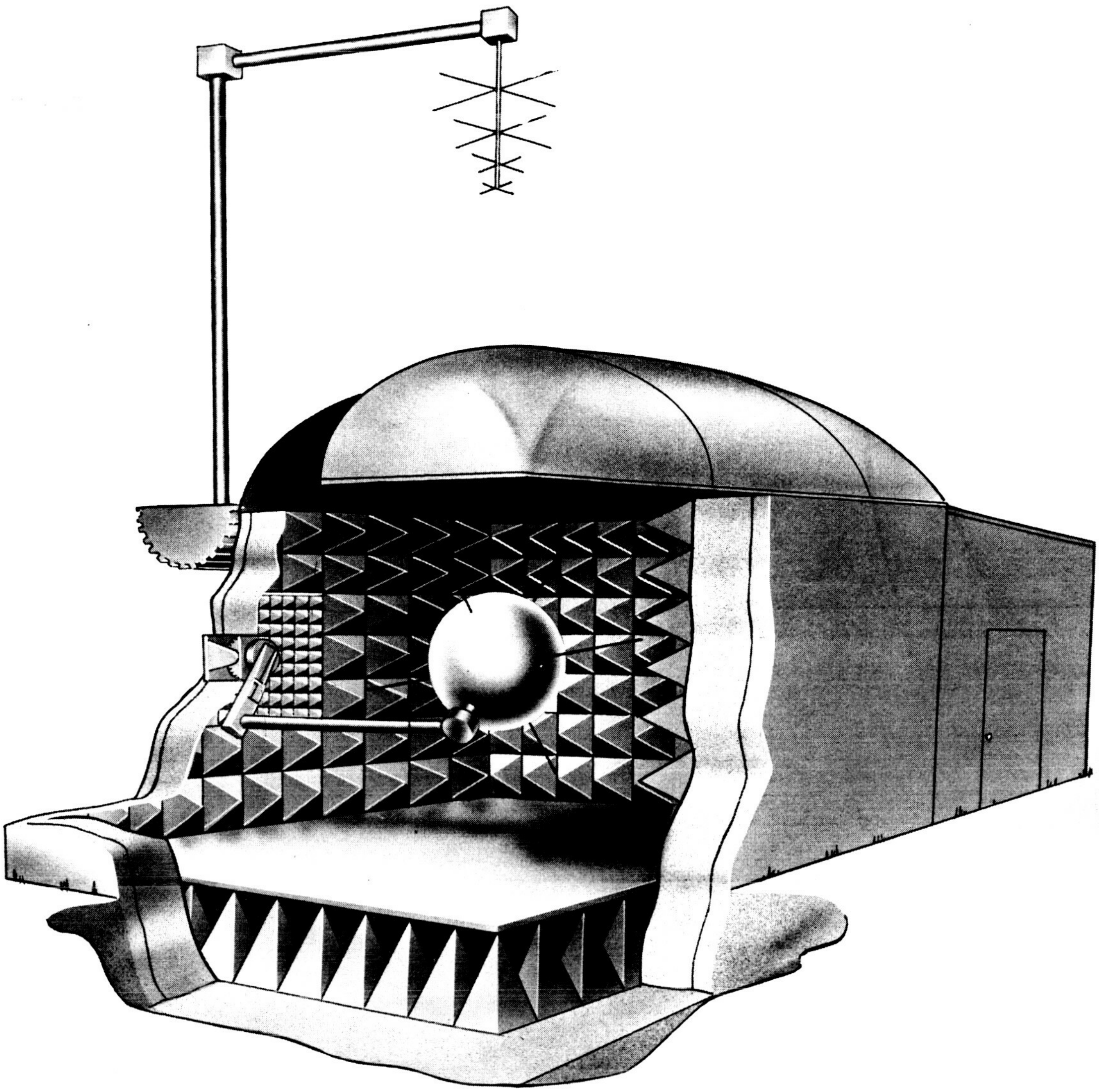

Figure 1–Vertical Anechoic Chamber

It should be remembered that an anechoic chamber is by no means free space. Therefore, it is of utmost importance that the RF anechoic chamber be "calibrated" not only as a function of frequency, but also as a function of illuminating or source antenna characteristics. Then, indeed, the confidence level at which the anechoic chamber may be used is defined.

Aubto

CONTENTS

## LIST OF ILLUSTRATIONS AND TABLES

# I. INTRODUCTION

## A. Antenna Test Range

The most important feature of an antenna test range is the control and reduction of reflections to the extent that they do not introduce significant errors in the measurement of the system under test. In order to achieve this, most test range sites are chosen in open fields clear of reflecting objects. Satisfactory operation is obtained as long as the system under test is sufficiently directive to discriminate against ground reflections and reflections from the test tower. Antennas for small scientific spacecraft are operated in the UHF refion and designed to be as nearly omnidirectional as possible and thus are a "worst case" for conventional test ranges. The ideal solution is to provide a reflectionless invironment for the system under test that still permits convenient operation.

Recent advances in r-f absorbent material has improved the performance of r-f anechoic chambers to where they are comparable to the best outdoor range sites.

## B. Definition of R-f Anechoic Chamber

A r-f anechoic chamber may be defined as an enclosure, suitably lined with an electromagnetic energy suppressing (absorbing and scattering) material, which may be used to measure such electrical characteristics as impedance, radiation pattern, and back scatter of a body within the chamber.

Further, the degree of suppression of reflected undesirable electromagnetic energy shall be such as to approximate free space. The allowable divergence from free space is a function of the type of test and the tolerable error which the disigner places on the test. For instance, a higher level of reflections may be tolerable when measuring impedance than when attempting back scattering measurements.

C. Testing Criteria as a Function of Type of Test: Impedance, Back Scatter, and Radiation Pattern

A primary requirement for measuring "free space" impedance of an an antenna is the exclusion of all external, foreign sources of reflection. This requirement at first thought appears extremely stringent, if not impossible. To meet the requirement explicitly would mean that an impedance measurement would have to be made at distances miles from the surface of the earth and from within the antenna system. Fortunately, the requirement can be relaxed to a degree governed by the tolerable error permitted in the system impedance expressed as a Voltage Standing Wave Ratio. Consider a perfectly matched antenna system radiating energy. Under a condition of no electrical mismatch from external sources there would be no standing wave and VSWR = 1.00:1. In practice, all antenna systems exhibit some mismatch from reflection resulting from electrical discontinuities. The vector addition of the incident and reflected voltages results in a standing wave, the magnitude of which is expressed in the familiar form:

$$\mathrm{VSWR}_{db} = 20 \log_{10} \frac{E_1}{E_2}$$

when

$E_1$ = incident voltage

$E_2$ = reflected voltage

This VSWR is an indication of the power transfer of an antenna system. For instance, a system with a VSWR of 6.0.1 would reflect 1/2 of the available power which is intolerable in most applications. Below is a brief table indicating the percentage of r-f power transmitted as a function of system VSWR.

| VSWR | R-f Power Transmitted |
|---|---|
| 1.00:1 | 100 % |
| 1.04:1 | 99.6 % |
| 1.22:1 | 99.02% |

Since a perfect impedance match is seldom achieved the question then becomes how large a reflection due to the environment of the test site is tolerable while still permitting acceptable measurement of reasonable accuracy of the system impedance. Consider first, a worst case condition, i.e., all the incident energy striking a reflecting surface is reflected back to the antenna under test. If the power radiated $P_0$ from a perfectly matched antenna of unity gain, travels a distance R to a reflecting wall and is completely

reflected back to the antenna a standing wave will result. However, the inverse square law for the attenuation of electromagnetic energy will reduce the amplitude of the reflected wave such that the SWR induced will be less than infinite. For example, the attenuation of a 136 Mc signal to a reflecting wall 8 feet away can be computed from:

$$\alpha = 37 + 20 \log f + 20 \log R$$

where

$\alpha$ = attenuation (db)

f = frequency (mc)

R = distance (feet)

then

$$\alpha = 23.53 \text{ db}$$

Assuming perfect reflection from the wall, the signal will be further reduced by 6 db in the return path to the antenna. Thus, the returned signal will be about 29.5 db below the incident signal. The resulting mismatch to the perfectly matched antenna is computed from:

$$|\Gamma| = \frac{r - 1}{r + 1}$$

where

$$|\Gamma| = \text{reflection coefficient} = 29.53 \text{ db} = .0335$$

$\therefore$ VSWR = r = 1.07:1

From the analysis above it is concluded that the impedance of a low gain antenna system may be measured with confidence if the walls of the enclosure are at least eight feet away and are less effective as a reflector than a metallic wall. Thus, the requirement on the absorption of unwanted reflections from the environment is easily met when making impedance or VSWR measurements on low gain antenna systems.

By definition, $\sigma$, the scattering cross section of a body is the ratio of the power scattered per unit solid angle to the power incident per unit area. In terms of the radar equation,

$$\sigma = \frac{P_R \, 16\pi^2 R^4}{P_T \, G_T G_R \, \lambda^2} \text{ square meters,}$$

where

$\lambda$ = the wavelength in meters.

$R$ = the distance between the source antenna and the scattering cross section body in meters.

$P_T$ = the transmitted RF power.

$P_R$ = the received (reflected) RF power.

$G_T$ = the transmitting antenna power gain with respect to an isotropic radiator.*

$G_R$ = the receiving antenna power gain with respect to isotropic radiator.*

The problem which presents itself in measuring scattering cross sections in an anechoic chamber is the suppression of the energy from chamber

*An isotropic radiator is a fictitious antenna, used as a reference, which radiates energy truly omnidirectional. Further, assuming this antenna is radiating an RF power of one watt, the magnitude of the electric field strength measured at a radius of 1 mile from the source is equal to 3.40mw/meter.

walls reflected back to a receiving antenna. The necessary chamber performance, as in the case of VSWR measurements in a chamber, is relative. For example, a large scattering cross section would reflect an energy level which could be many orders of magnitude greater than energy contributed by the reflected energy from the chamber walls (including ceiling). In this case a percentage tolerance error can be established. Unfortunately, many radar cross section measurements are made of objects which have a small scattering cross section. Now, although the walls of the chamber absorb and suppress the RF energy, the fact that the walls are many orders of magnitude in size larger than the object being measured results in a chamber wall reflection coefficient which is as large as or larger than the object to be measured. In other words, the scattering energy of the body to be measured is hidden by the reflections from the chamber.

There is one technique which is described by Elery F. Buckley (Emerson and Cuming, Inc.) which allows a calibration of a chamber for measuring radar cross sections in a controlled manner.

Very briefly, a transmitting and receiving antenna are placed at one end of a chamber. Two or more conducting spheres of known physical size (and hence known radar cross section) are placed at the opposite end of the chamber one at a time. The spheres, one at a time in the chamber, are rotated eccentrically about an axis producing an in-to-out of phase response. There will be two amplitude components for each of the different size spheres

which contribute to the recorded interference pattern. One of the amplitude components is from the sphere; the other is the constant field equal to the energy return from the chamber plus electric field from transmitter-receiver cross coupling. The voltage ratio of these magnitudes produce an ambiguity. That is to say, the chamber scattering cross section will be either of two values, hence, the second measurement is made using a different conducting sphere with a known $\sigma$. The second measurement results again in two values of the chamber cross section. The true chamber reflecting cross section is that cross section which is common to both of the measurements.

An example which illustrates the magnitude of energy suppression which an anechoic chamber must exhibit for the measurement of radar cross sections follows:

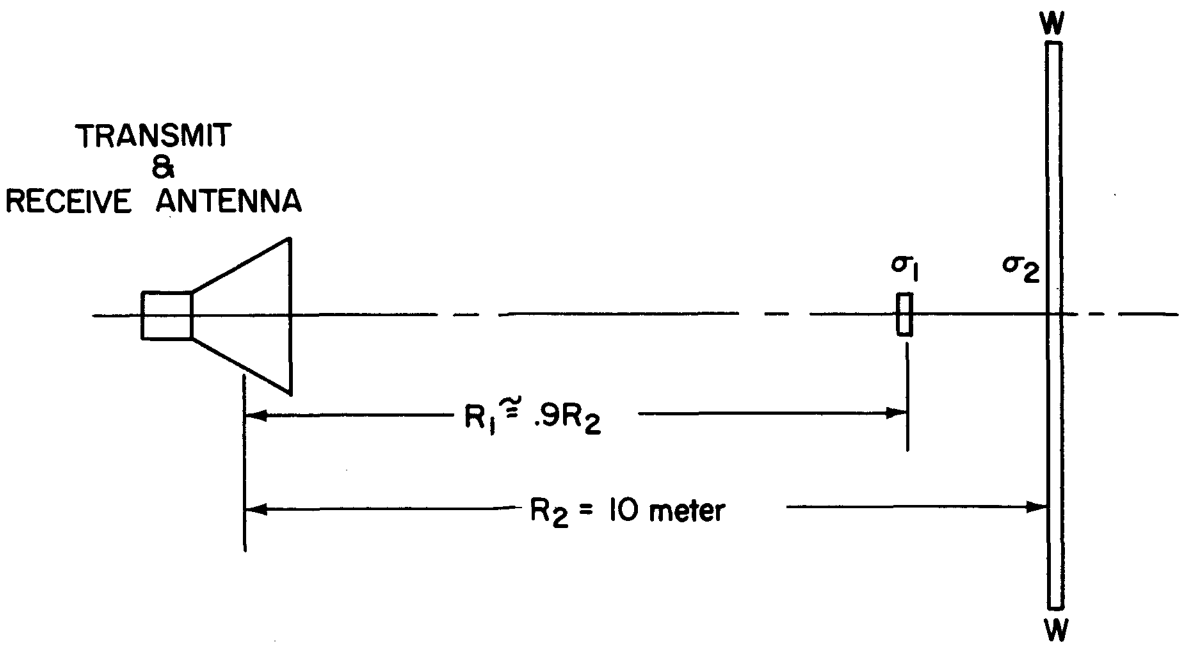

Let the scattering cross section be that produced by a sphere of radius $a = 0.1$ meter when the wavelength $\lambda = 3$cm (i.e., $a/\lambda > 1$). Then the scattering cross section $\sigma_1 = \pi a^2 = 3.14 \times 10^{-2}$ meter$^2$

Now, the return power received by an antenna $G_r$ from a scattering body of cross section $\sigma$ when the transmitted power $P_T$ is radiated by an antenna $G_T$ is,

$$P_R = \frac{P_T \; G_R \; G_T \; \lambda^2}{16\pi^2 \; R^4} \sigma$$

Consider first the return power received from the spherical scattering body and letting $P_T = 1$ watt, $R_1 = 9$ meters,

$$G_T = G_R = 63 \text{ and } \lambda = 3 \text{ cm.}$$

P

$$P_{R1} = \frac{P_T \; G_R \; G_T \; \lambda^2}{16\pi^2 \; R^4} \sigma_1$$

$$P_{R1} = .109 \times 10^{-6} \text{ watts}$$

Next, assume the wall w-w in the figure on page 7 to be a perfectly reflecting surface 3 meters on a side so that the wall radar cross section is

$$\sigma_2 = \frac{4\pi \; A^2}{\lambda^2}$$

where $A$ = area of wall and $\lambda$ = wavelength at the operating frequency.

Then,

$$\sigma_2 = \frac{4\pi \; A^2}{\lambda^2}$$

$$\sigma_2 = 12.56 \times 10^4 \ M^2$$

The return power received from the back wall w-w is (the side, top and bottom walls may be neglected in this case since the predominant contribution to erroneous back scatter measurements is the back wall),

and, $P_{R_2} = .284$ watts

By comparison $P_{R_1}/P_{R_2} = -64.2$ db

Or, the energy normal to the back wall W-W must be suppressed by 64.2 db to allow the spherical body (.1 meter radius) to present an equal amplitude to the receiver antenna $G_R$. Of course, further suppression of the back wall energy must be attained before the energy from the spherical body is discernible from (i.e., above) the back wall scattered energy.

The example outlined above now allows a feeling for the nature and magnitude of energy suppression and/or absorbing characteristics that may be required of an RF anechoic chamber designed to measure radar cross sections.

Measurement of antenna radiation patterns generally requires a better anechoic chamber than one for the measurement of antenna impedance. But the requirements are not as critical as for radar cross section (back scatter) measurements.

As an illustration, let us examine a typical E-plane pattern of a horn antenna and then show the effects of various magnitudes of reflected energy interfering at various aspect angles in the chamber. Figure 2 shows the

E-plane pattern as measured in a controlled environment at an outside antenna range. The pattern approaches the theoretical pattern for a horn antenna exhibiting uniform distribution across the aperture. Figure 2 also shows a ray outline of reflected energy when measuring the E-plane pattern of this antenna in an anechoic chamber. Let sources of reflection be located at angles defined by $\theta$ = 50° and 60°. Then the resulting perturbations from these reflecting sources are shown in Figure 2 as dashed lines. The deviations in the pattern are identified as 1 , 2 , and 3 . The magnitude of the perturbation at 1 is 1.6 db. The magnitude of the reflected energy from point I which produces this 1.6 db is equal to 21 db since the reflection coefficient in db = 20 log (S - 1/S + 1), where S = standing wave ratio. Refering to the figure, it can be seen that the perturbations take place at -14.2 db on the radiation pattern. Therefore, the actual reflection coefficient (magnitude of the interfering reflected energy) is equal to 35.2 db. At point 2 the deviation from point II is 1.1 db or a reflection coefficient of 25 db. Since the radiated energy is down 15.5 db at this point, the actual reflection coefficient is 40.5 db. Now consider point 3 (i.e., 0 db down on the pattern). A refection coefficient of 40 db will cause a 0.175 perturbation in the pattern at this point.

From the above exercise one can now see clearly the effect of reflected energy on a typical pattern from arbitrarily chosen points in an anechoic chamber enclosure which is 35 db to 40 db down from the incident energy.

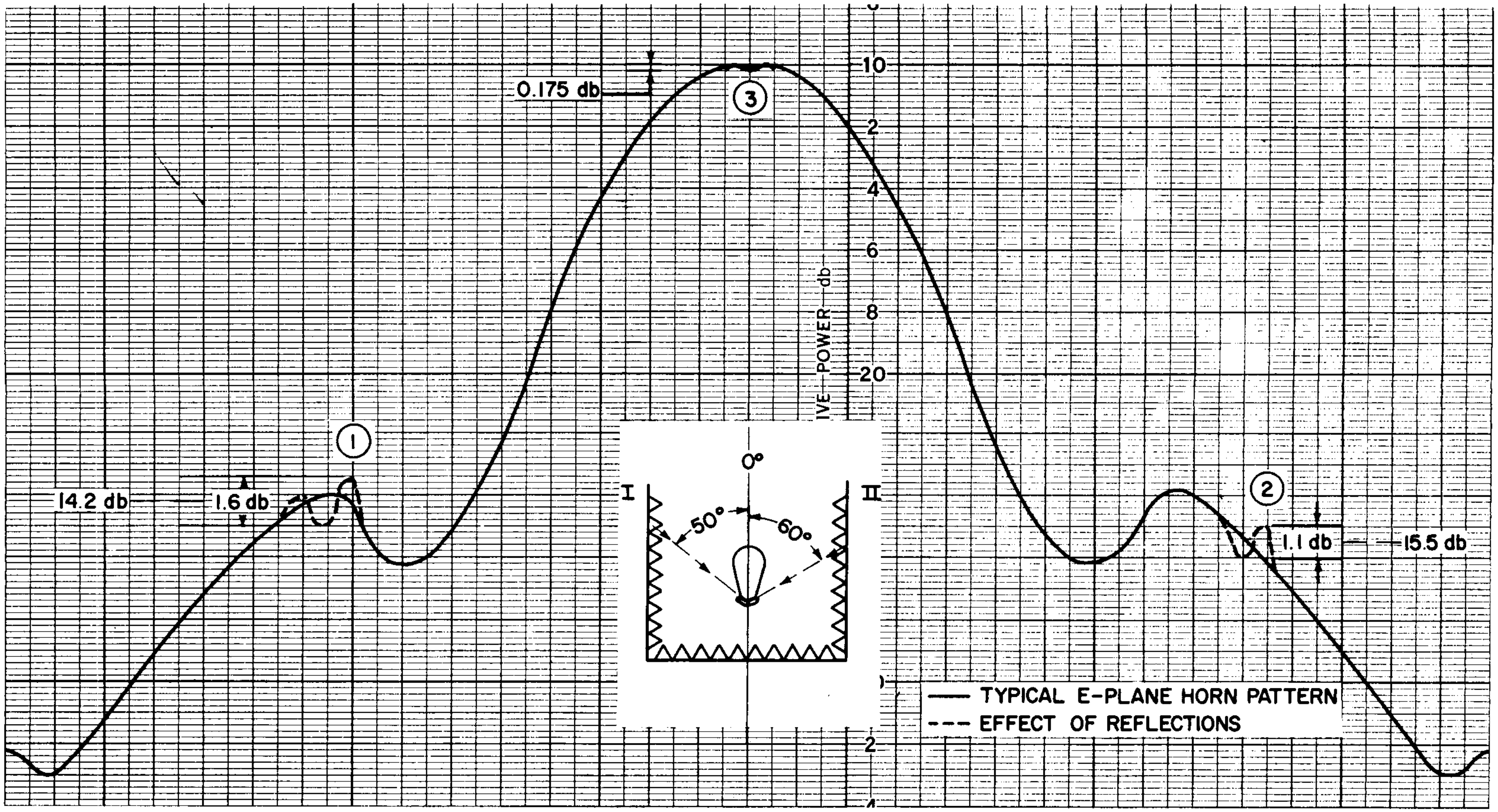


Figure 2-Effect of Reflected Energy on Typical E-Plane Pattern of Horn Antenna

## II. DESCRIPTION OF VERTICAL RF TEST RANGE

### A. Physical Description

The vertical test range is as shown in Figure 1. The walls and floor of the structure are reinforced concrete. Attached to the chamber through a common wall is the control room which houses all the electrical measuring devices. Opposite the control room side are two doors which when opened allow the chamber to be used as one end of a horizontal antenna range in conjunction with available antenna towers. The roof of the chamber is an A-sandwich type RF transparent radome. Also, shown in this figure is the outside azimuth - elevation mount and fiberglas mast approximately 35 feet above the chamber controlled from inside. This facilitates the changing of source antennas. Inside the chamber (see Figure 3) is a wall-mounted antenna mount capable of rotating and allowing measurement of a satellite antenna system at or near the center of the chamber quiet zone.

The walls are lined with pyramidal absorbent material 70 inches in length on 2 feet square bases (Figure 4). In the area of the side wall mount smaller pyramidal absorbent material is used allowing the rotation of an off-set arm containing the fiberglas mast. The floor of the chamber is lined with foam structure 70 inch pyramids on top of which is cemented a smooth floor - decking material of 1/2" thick sheets of semi-rigid vinyl foam which can be walked upon in setting up experiments within the chamber.

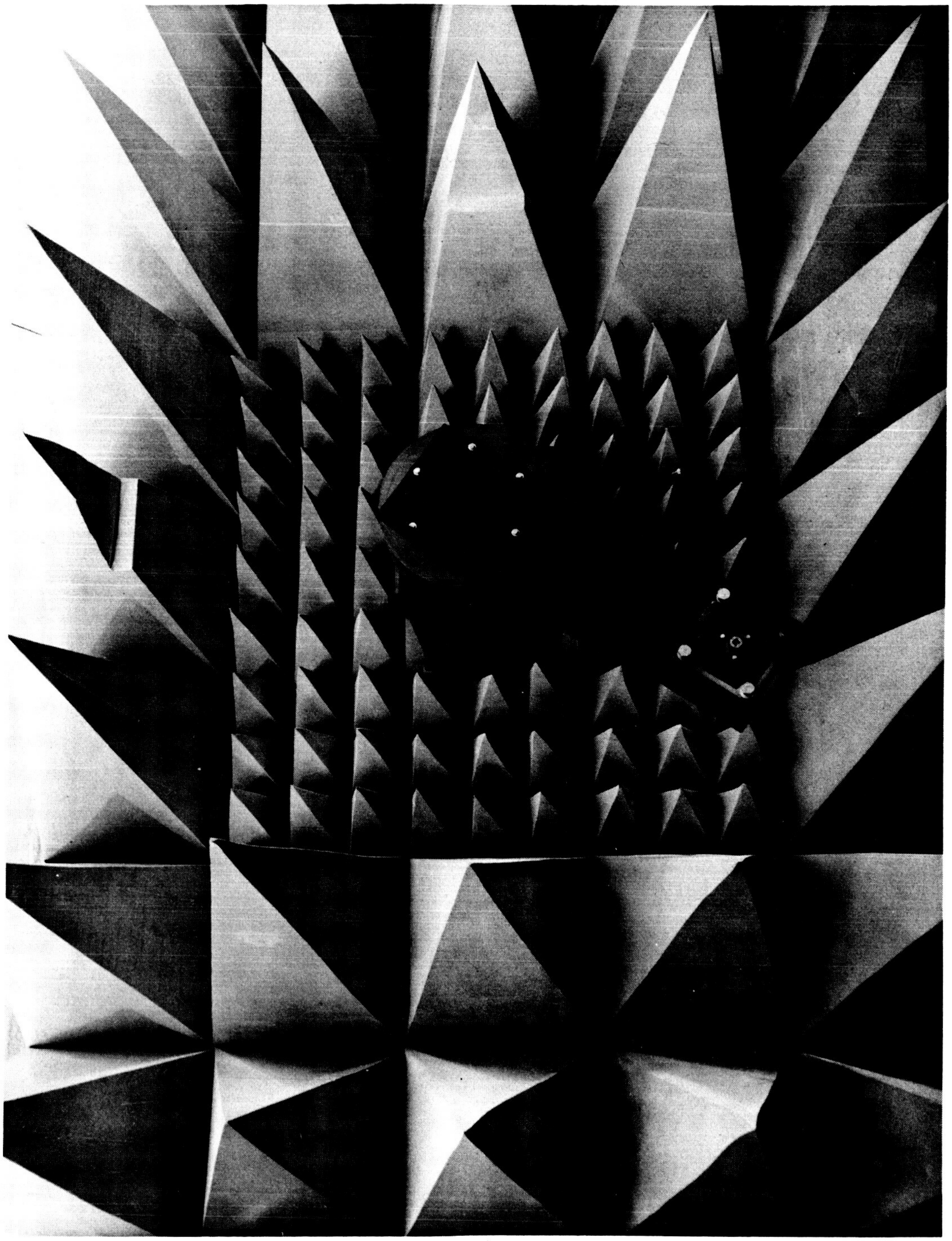

Figure 3-Photograph of Wall Mount Inside Chamber

Figure 4–Photograph Illustrating Size of Absorbent Material

The radome is a structural body of the A-sandwich type. It is approximately 4" thick and the 9 sub-pieces are assembled into a continuous weather protective roof (Figure 5).

Uniform chamber lighting is achieved by directing four flood lamps toward the radome. The four lamps are located at the four upper corners of the chamber such that they are well hidden by the absorber on the walls. This technique of lighting results in two very favorable conditions; the lighting is uniform and avoids the visual problem of looking into the lamps; a minimum of RF reflection from the fixtures is obtained since they are well shadowed by the 70" absorbent material.

Finally, the chamber is temperature controlled to prevent large variations of temperature which may effect antenna measurements.

B. Electrical Description

Electrically the chamber was lined on 5 surfaces with an RF absorbent material and the 6th side enclosed by an RF transparent (radome) roof.

The RF absorbent material was supplied by the B. F. Goodrich Company, Shelton, Connecticut. Each individual piece of the material, VHP-70 is a 70" high pyramid shaped absorber on a 2 feet square base. All of the absorbent material exhibits a minimum reflection coefficient of 28 db at 120Mc, 40 db at 400Mc and 50 db at 1,000 to 10,000Mc.

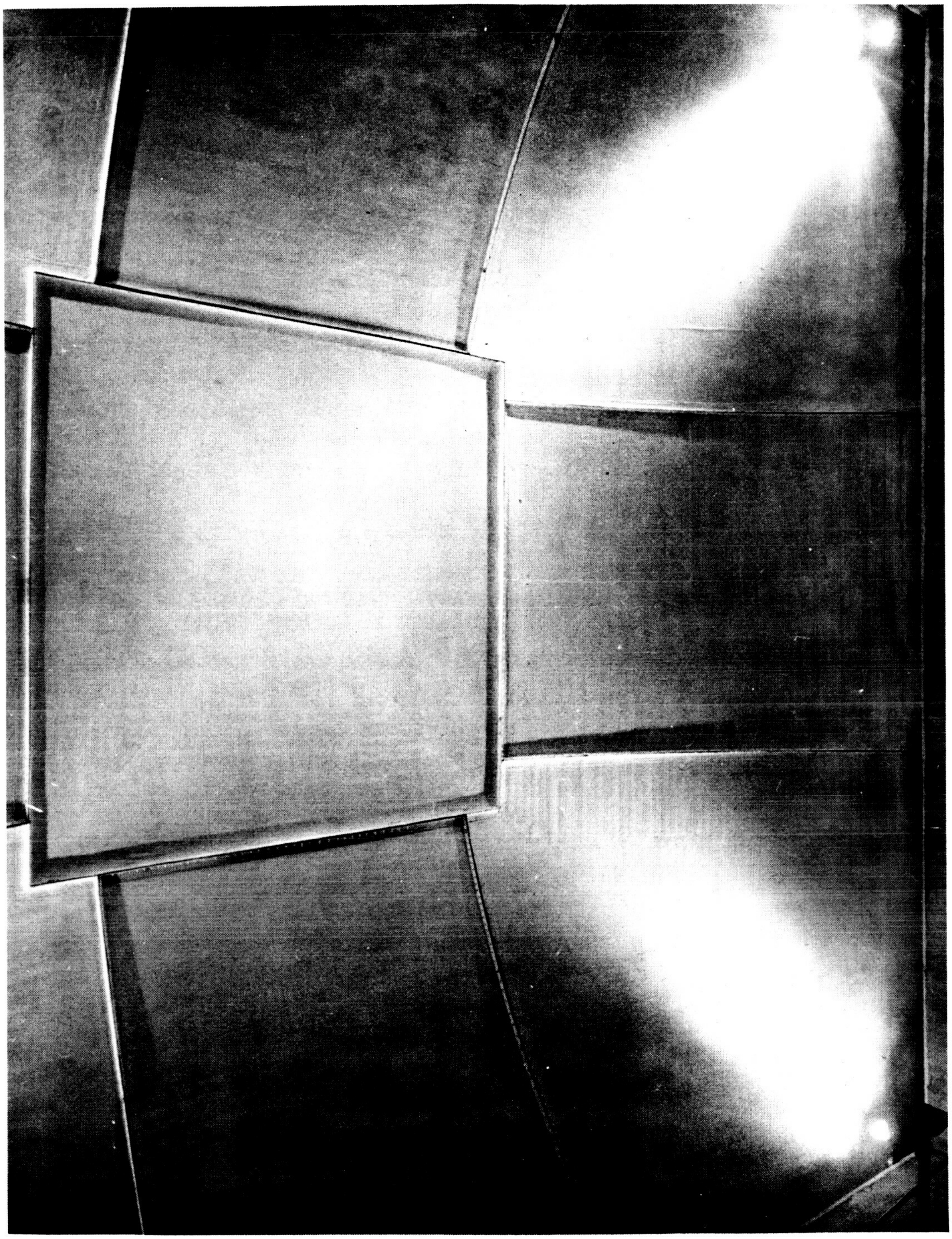

Figure 5–Photograph of 9 Panel Radome

The tests on the absorber at the manufacturer's plant were made in a closed loop technique at 120Mc and 400Mc. At 1,000, 5,000 and 10,000Mc an open loop technique was used. The closed loop technique consisted of measuring four 2'×2' absorber pieces at a time in a flared waveguide system in which the absorbent material serves as a load under test. The absorber is moved inside the waveguide resulting in a standing wave that moves in conjunction with the physical movement of the absorber. A fixed probe inside the waveguide located between the absorber and RF oscillator detects the standing wave which is converted to power reflected.

The open loop technique of testing consisted of a horizontal version of the NRL type arch method. A reference was used which consisted of a flat 2'×8' metal plate. The reflection level of four 2×2 pieces was measured and compared to the flat metal plate. The reflectivity of the absorbent material is the difference in return power in db between the metal plate and the absorbent material.

The radome was supplied by Raymond Development Industries, Inc., Huntington Park, California. The electrical characteristics of the A-sandwich radome material were specified as:

(a) Transmission loss $\leqq$ 7.5% over the frequency range of 120Mc to 10,000Mc.

(b) Refraction less than 10% for angles of incidence from 0° to 45°.

(c) Loss tangent of glass laminate = .005.

(d) Dielectric constant of glass laminate = 4.0.

(e) Loss tangent of foam core = .0005.

(f) Dielectric constant of foam core = 1.12.

Although tests at the manufacturer's plant confirm the meeting of the specifications on a flat 40"×40" sample of the radome, measurements indicate that the actual radome does exhibit less than specified performance particularly at frequencies above 1,000Mc. This can be easily explained since the actual completed radome psssesses a curved surface and the nine pieces comprising the total radome are assembled with beefed-up glass laminate flange sections. These two conditions increase the detrimental effects (increased diffraction and reflection).

As previously stated the frequencies of primary interest are in the 120Mc to 400Mc region. But some tests were performed in the chamber at higher frequencies.

Normally, in evaluating the chamber a quiet zone is defined. That is, a volume within the chamber in which known (measured) reflectivity levels exist. Then in this zone antenna systems can be evaluated being fully aware of the limitation of the chamber. Therefore, by definition, the quiet zone is a 10 foot diameter sphere which is tangent to the chamber floor and centered elsewhere within this chamber.

## C. Advantages

Ground reflections are the most serious source of error when using a conventional test range for measurements of low frequency, low-gain antennas. The error may be refuced to a degree by additional height to the towers, but towers over 100' high are expensive and rather inconvenient to use. Likewise a conventional anechoic chamber designed for operation at low frequency is expensive and requires a large building to provide even a modest size test range. The vertical test range provides an attractive compromise between tall towers and a large anechoic chamber. The chamber portion need only be large enough to prevent reflections from the ground and nearby reflecting surfaces and the tower need only be tall enough to hold an antenna out of the near field of the antenna under test. Furthermore, the length of the test range may easily be varied by adjusting the height of the outside antenna. Operation of a vertical range is especially convenient. The model under test, the test and control equipment, and personnel are all at ground level and thus avoid the need for hoists and elevators.

# III. ANALYSIS OF CHAMBER

The magnitude of unwanted reflections that can be tolerated in an antenna test range have been shown to be a function of the parameter being measured. Since the site is never perfect, the results obtained may be interpreted in terms of the known site imperfections provided the reflection coefficients and in some

cases phase are accurately specified. However, measurement of reflection coefficient of absorbent material is difficult and techniques for its evaluation have not been standardized. Currently the Pattern Comparison Technique[1] and the Free Space VSWR Technique[2] are favored in evaluation of r-f anechoic chambers. In both techniques the significant result is the comparison of the incident to the reflected energy from an absorbing wall to determine its reflection coefficient.

Briefly, in the Pattern Comparison Technique, the pattern of a directive antenna (15 to 20 db gain) is measured successively at closely spaced points along the radii of the chamber quiet zone. The quiet zone may be defined as the volume within an anechoic chamber in which an antenna under test will be measured. Then the patterns are superimposed on each other with pattern peaks coincident. The deviations in the patterns are read at different aspect angles and VSWR curves vs aspect angle are constructed. The curves may then be converted to reflection levels within the chamber.

The Free Space VSWR Technique is a method of continuously recording the amplitude variations produced by reflections. Two directive antennas are used, with one being moved continuously across the chamber quiet zone at a discrete aspect angle for each recording. The amplitudes recorded are reduced to incident and reflected energy levels, thus allowing the reflection coefficient vs aspect angle of a chamber to be determined.

From the brief summary above (and more so from the referenced literature) it can be seen that both techniques rely on use directive antennas. This is not

a disadvantage in the usual situation where the chamber is large in terms of wavelength and directive antennas are usually evaluated. However, in the vertical test range more emphasis is placed on measurement of nearly omnidirectional antennas in a termination chamber that is electrically small, i.e., approximately $1\lambda$ in depth and $2\lambda$ on a side. Although evaluation of chamber performance using directive antennas will indicate both a direction and reflection coefficient for sources of reflections, unless considerable effort is made to integrate the reflection levels from all directions the chamber will appear better than when used with an omnidirectional antenna. Therefore most of the analysis of both the scale model and the full scale range was made using a dipole antenna to probe the energy levels within the termination chamber. In this method, a dipole antenna is moved throughout the quiet zone and energy levels vs position recorded. The difference between the levels recorded and calculated free space levels are converted into VSWR and finally a reflection coefficient computed.

It is common practice to try to reduce the large number of different reflection coefficients that are measured in evaluating a chamber to a single number that is then used to define the chamber's performance. In general, it will be found that this number is not really a common denominator and that the relative performance of two different chambers should not be judged on this alone. For instance the quiet zone of chamber A may be only 1/3 the volume that was included in evaluation of chamber B, yet chamber B may be considerably better than A over

the same quiet zone. Unfortunately, the performance rating of anechoic chambers is like the evaluation of radio receivers in 1940, i.e., not complete unless the test conditions are known as well as the results.

A. Scaled Chamber Measurements

Reflection coefficient measurements were made in a 1/9th-scale chamber. A photograph of the scale chamber is shown in Figure 6. Figure 7 defines the test set-up. No attempt was made to design and test a 1/9th-scale radome because the radome would appear as a thin wall structure in the frequencies of most interest (up to around 400Mc) in the full scale chamber. Although no scaled radome measurements were made in this particular chamber design it is felt that general comments on scaled radome measurements are in order.

Scaling a multi-panel, sandwich radome is, in general, difficult. Extreme care must be taken in scaling the ribbing, flange design and radome curvature. Serious errors can be expected if this precaution is not taken. Thin wall structural radomes of dielectric constants of approximately 3 or 4 may be scaled for measurements with confidence and also thick wall foam radomes of low dielectric constants ($\epsilon_n = 1.1$ to $1.4$) are practical for scaling purposes.

Measurements were made at frequencies from near 1,080Mc to 3,600Mc. This corresponds to full scale chamber measurement of approximately 120Mc

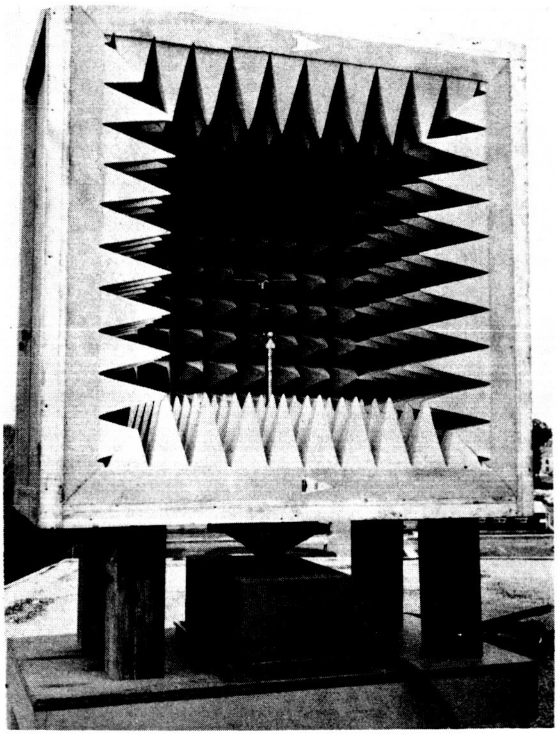

Figure 6–Photograph of 1/9th Scale Chamber

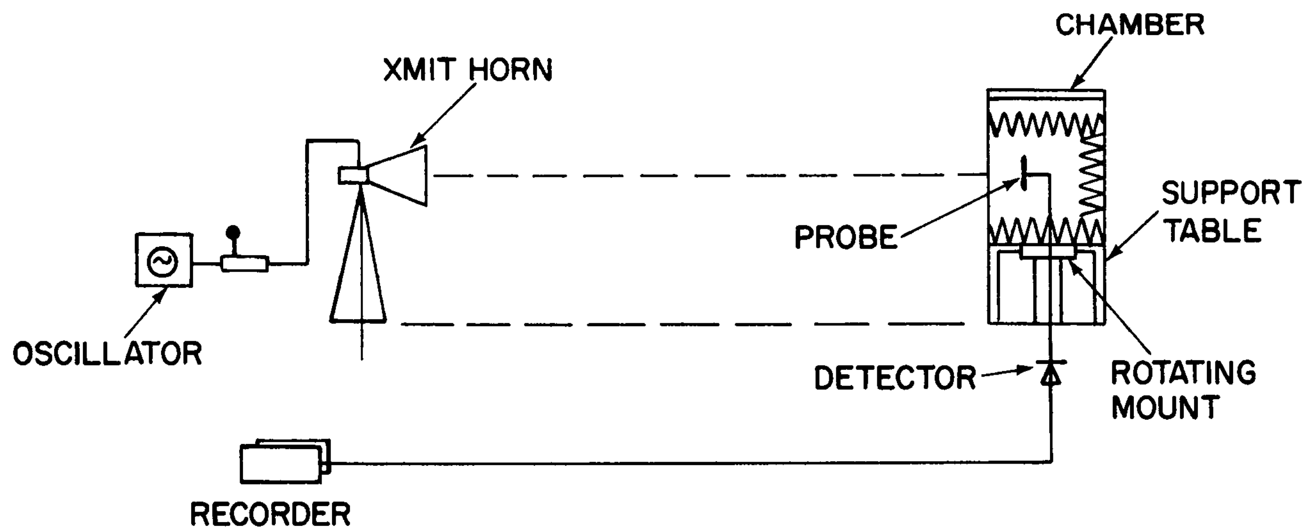


Figure 7–Equipment Set-Up for 1/9th Scale Measurements

to 400Mc. It is to be noted that a dipole probe is used inside the scaled chamber to deliberately prevent discrimination against any reflected energy. A directive type antenna would have been too selective.

The measurements at 1,080Mc in the 1/9th-scale chamber indicated a reflection coefficient of 20 db and at 3,600Mc 30 db reflection coefficients were measured.

Figure 8 is typical of the standing waves measured by probing the scaled chamber with dipoles. The dipole probes were moved in small increments in terms of wavelengths from the aperture of the chamber to the back. Figure 9 depicts standing wave curves resulting from probing across the chamber in small increments. This data is typical of that obtained in the 1/9th-scale chamber.

It was from these measurements that the full-scale chamber performance was predicted.

As was previously mentioned no attempt was made to determine the effect of an A-sandwich type radome on the full scale chamber at scaled frequencies. That the radome effect would be negligible at the low frequencies of interest was predicted on the basis that the radome would appear as a thin wall (approximately $\lambda/8$ thick or less) at 400Mc and lower.

## B. Full Scale Chamber Measurements

The quiet zone of the chamber was probed with a dipole using an illuminating antenna which was directional in nature.

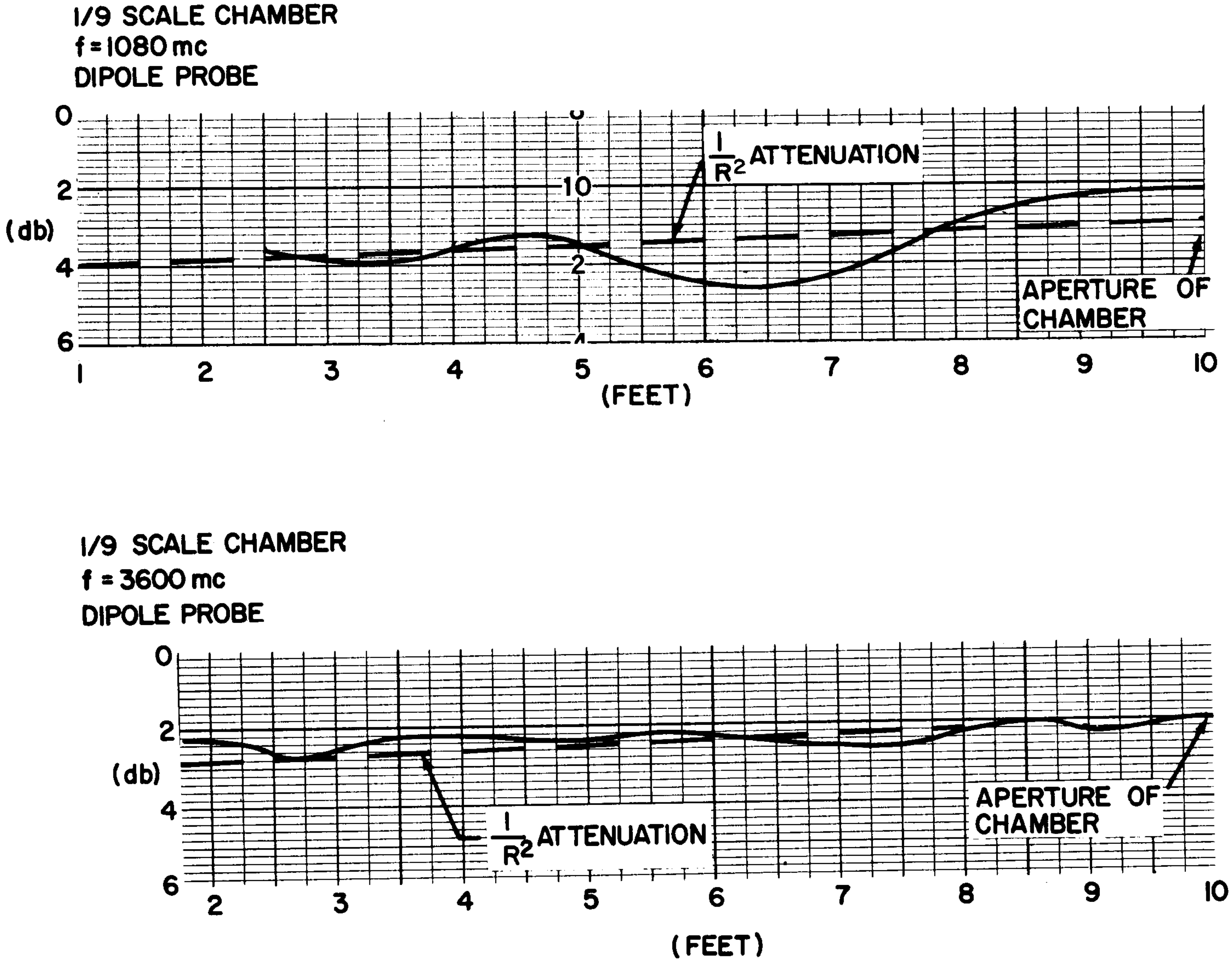


Figure 8-Standing Waves in 1/9th Scale Chamber Measured from Aperture of Chamber Floor

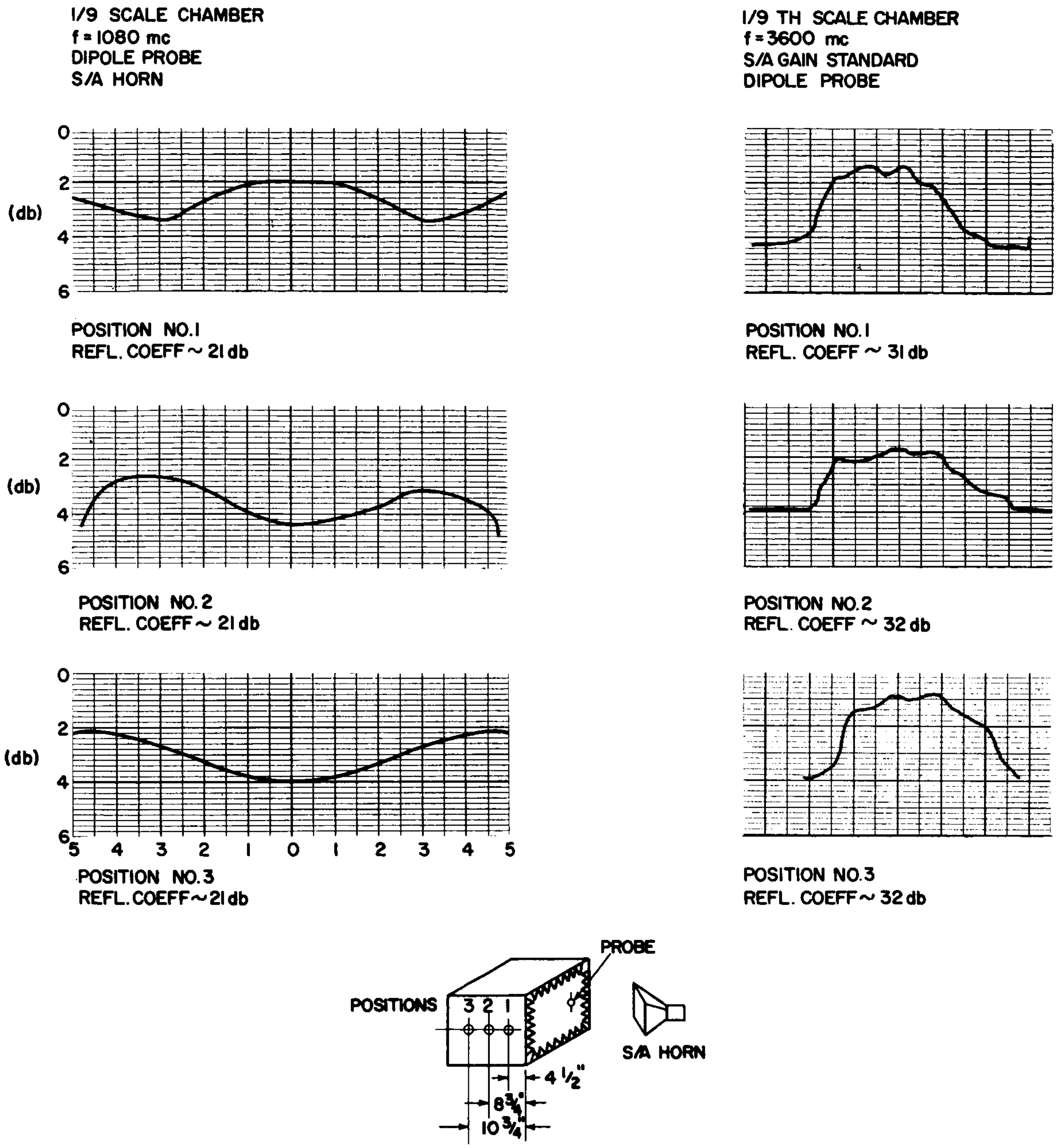


Figure 9–Standing Wave Curves Measured Across 1/9th Scale Chamber Aperture

Specifically, at 125Mc and 400Mc the magnitude of the reflection coefficient was determined by moving a dipole horizontally inside the chamber in directions normal to each wall and across the diagonals. With the dipole fixed to a cart made of low dielectric constant foam material, the cart was moved along tracks which could be oriented as desired within the chamber. The track, cart and dipole support are shown in Figure 10. There horizontal measurements were made at discrete heights of 2 (and/or 3), 4, 5, 6 and 8 feet above the floor of the chamber. The reflection coefficient in the vertical direction was determined by measuring the standing wave as a function of vertical movement of the dipole from 2 to 10 feet above the floor. Resulting standing wave curves are converted to an equivalent reflected energy level (reflection coefficient). Figure 11 is a typical curve. The dashed curve of Figure 11(b) represents the probed energy level as measured in Figure 11(a) in the absence of reflected energy. The solid curve superimposed on the dashed curve represents the effect of the reflected energy. Peak to peak value of the standing wave is 0.5 db. This standing wave of 0.5 db results from a reflected energy level of 30 db below the incident signal level. Or, Reflection Coefficient = 20 log VSWR-1/VSWR+1. Measured curves are shown in Figures 12(a) through 12(d).

At 1,200Mc reflected energy levels greater than expected were measured (approximately 32 db average). Also, the reflected energy levels were polarization sensitive (i.e., E-perpendicular vs E-parallel) with differences in

Figure 10–Photograph of Track an d Cart Arrangement

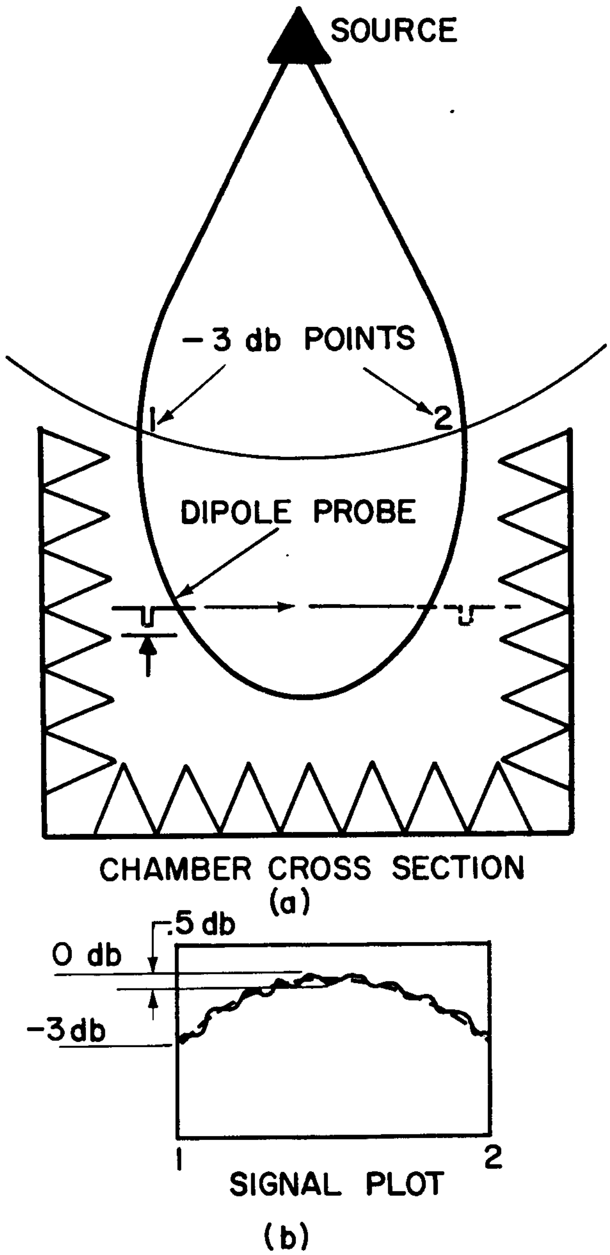


Figure 11—Interpretation of Standing Wave Curves

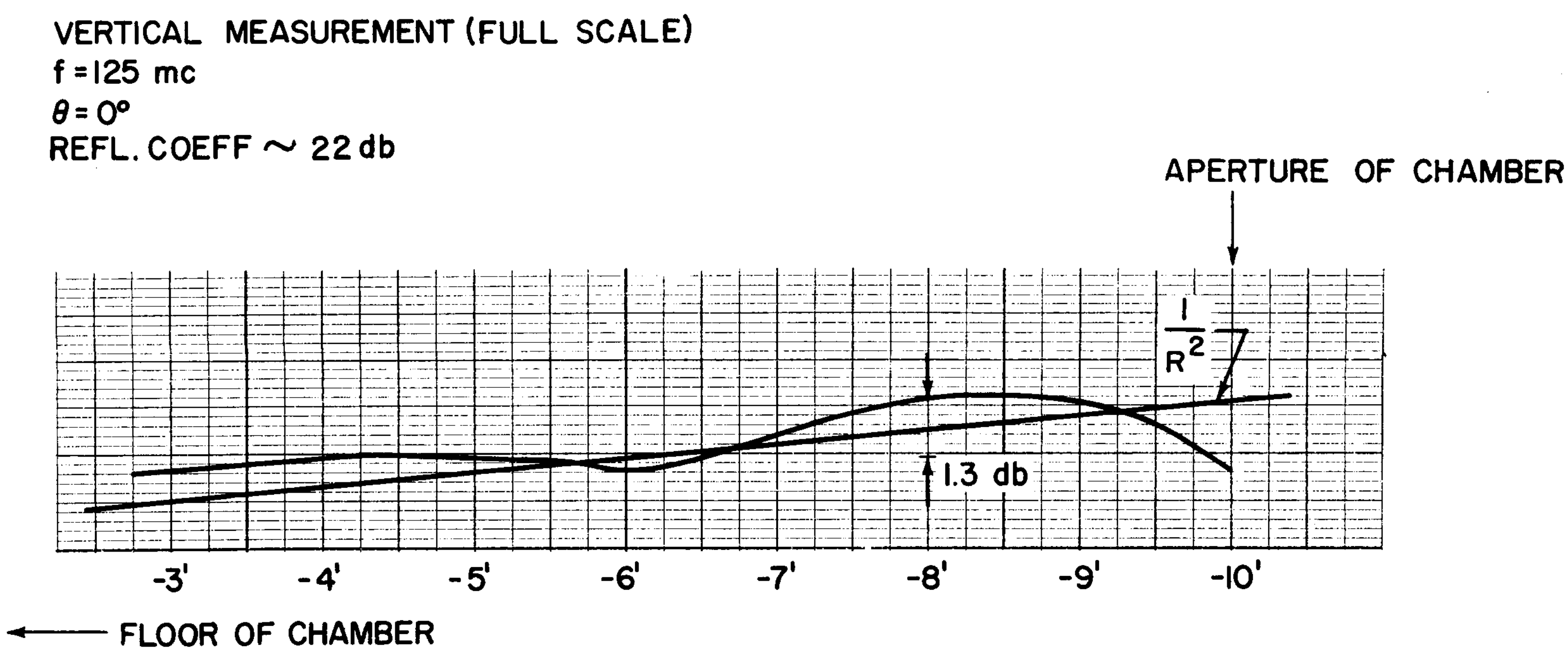


Figure 12a–Full Scale Chamber Standing Waves at 125 Mc, 400 Mc

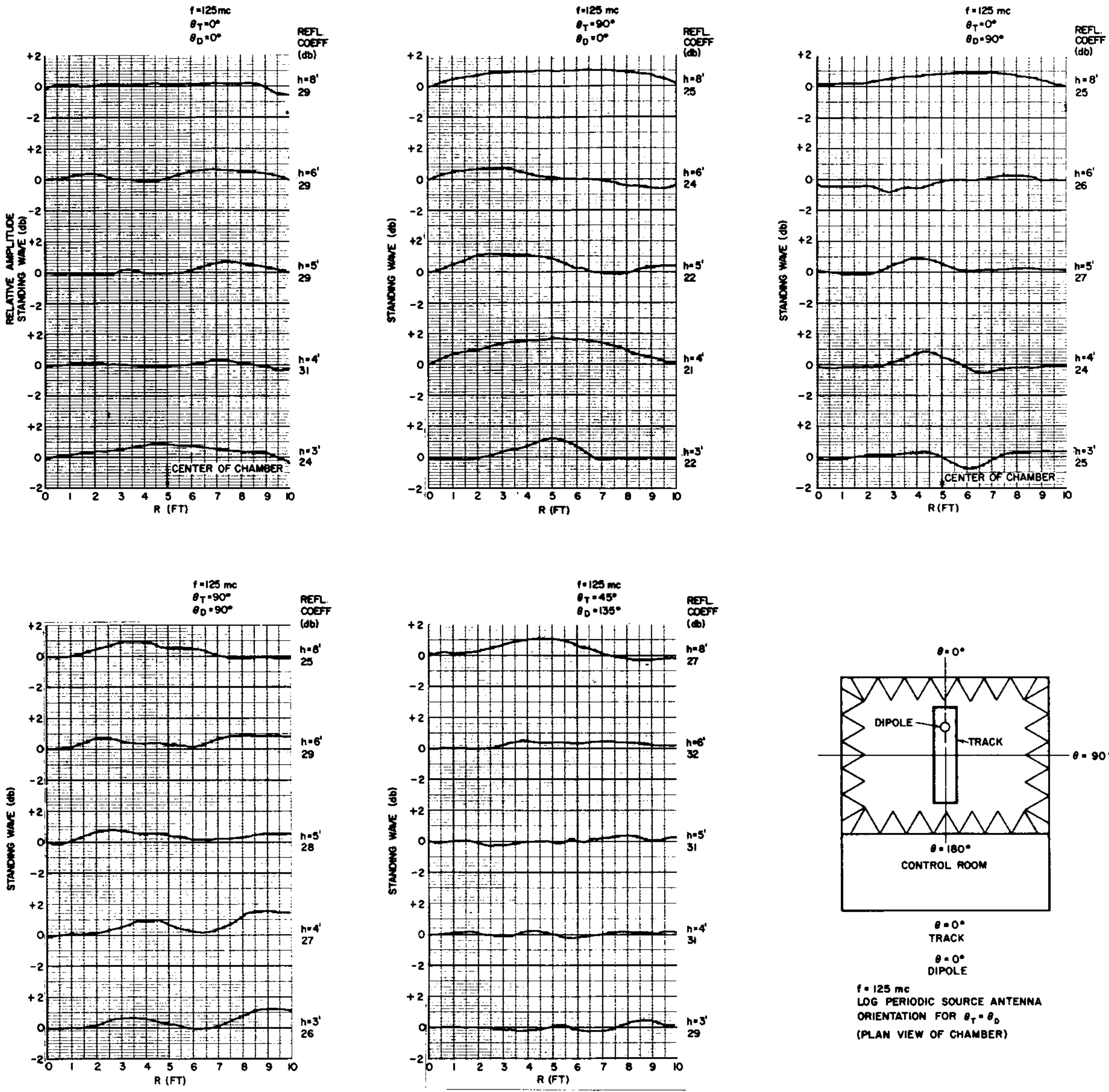


Figure 12b—Full Scale Chamber Standing Waves at 125 Mc, 400 Mc

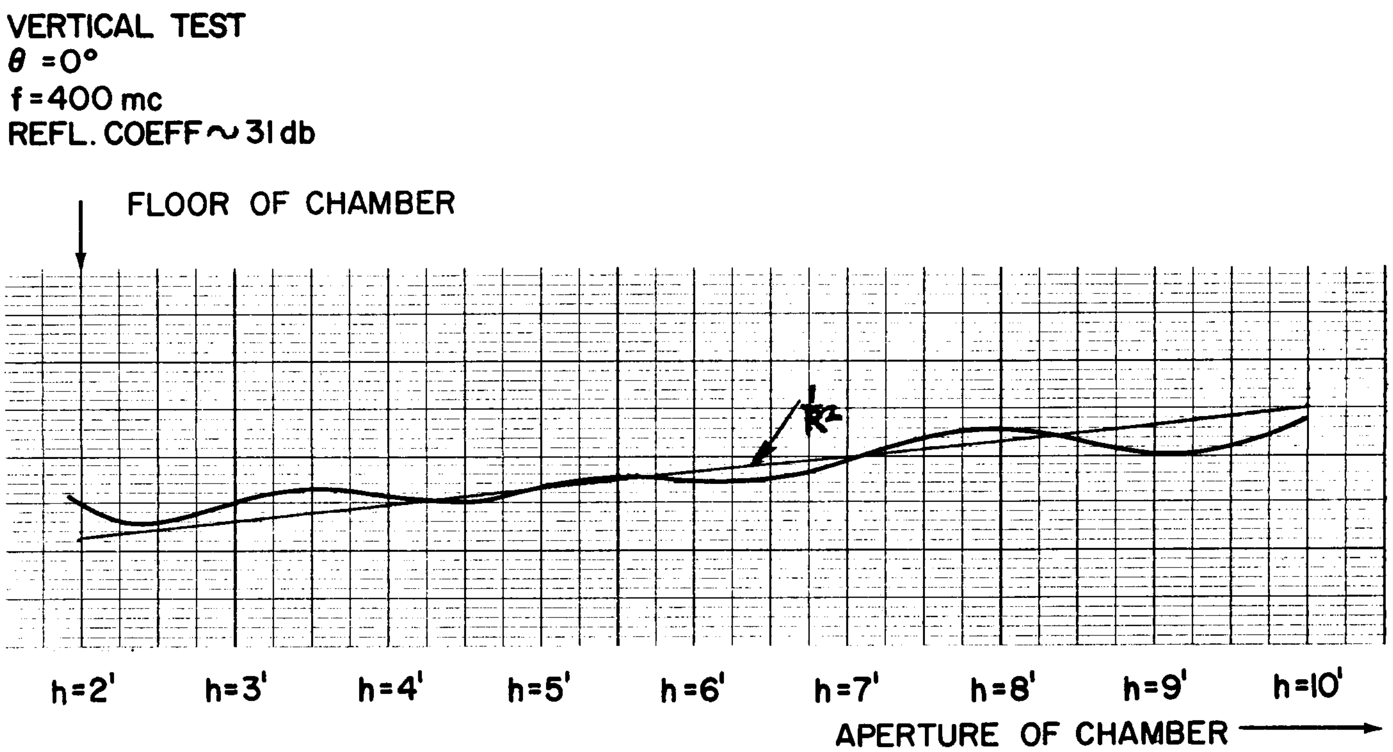


Figure 12c–Full Scale Chamber Standing Waves at 125 Mc, 400 Mc

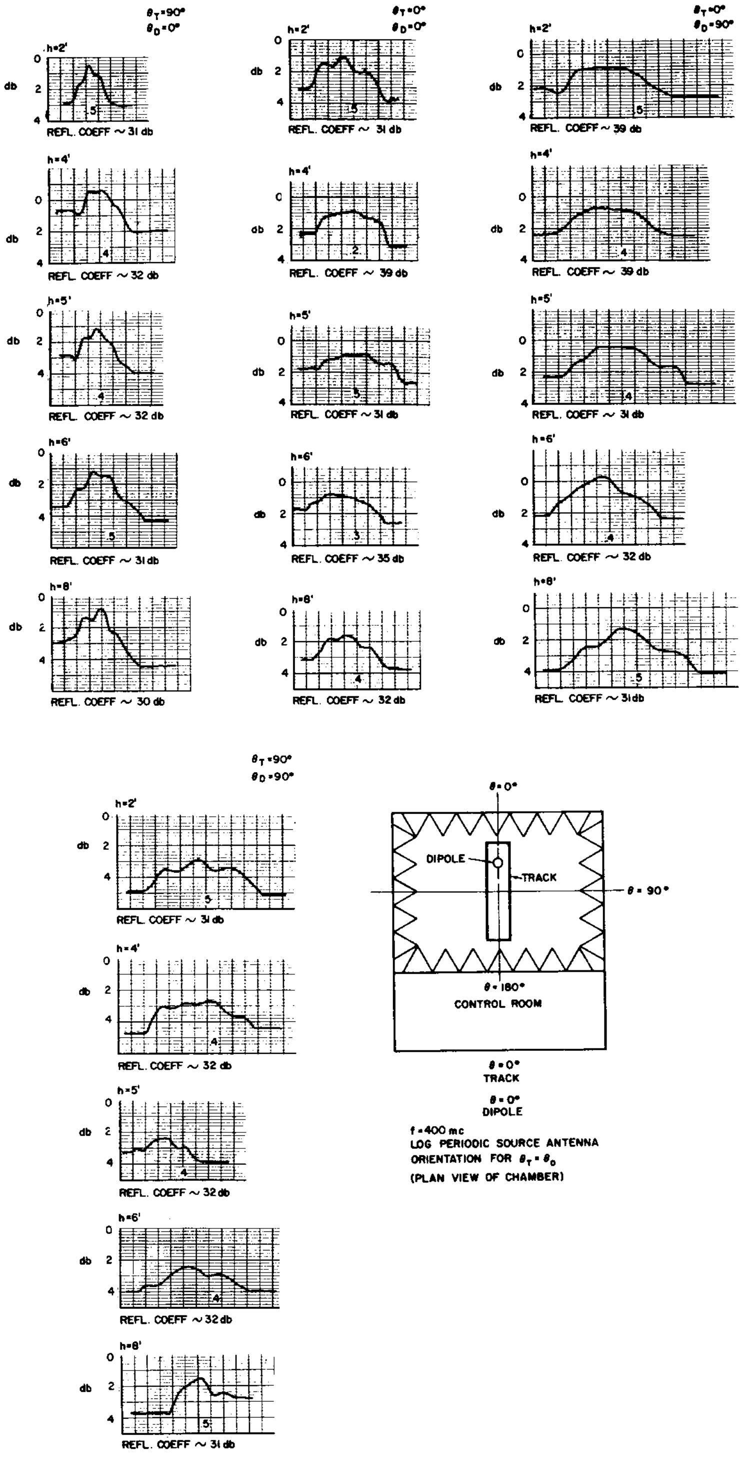


Figure 12d—Full Scale Chamber Standing Waves at 125 Mc, 400 Mc

reflection coefficients between 6 and 15 db as a function of aspect angle. This obvious deviation from the 45 to 50 db levels anticipated was attributed to the radome for two reasons:

(1) The chamber at 1,200Mc is electrically large ($15\lambda \times 15\lambda$ $10\lambda$) and therefore the chamber would be expected to be much better than at 400Mc (reflection levels $\approx$32 db).

(2) This A-sandwich radome (4 inches thick, with solid fiberglas panel flanges) appears as a relatively large discontinuity.

Measured magnitudes of reflected energy for various linear polarization orientations when probing the chamber at 125Mc and 400Mc are tabulated in Tables 1 and 2. Some inconsistency is apparent, especially in the higher coefficient values measured at 125Mc. This is attributed to instability of the measurement equipment; however, retests of selected orientations indicate no serious differences from the data presented or the conclusions drawn from the data.

Table 1

125Mc Chamber Reflectivity Levels

| Track Orientation $\theta_T$ | Dipole Orientation $\theta_D$ | Dipole Height Above Floor | | | | |
|---|---|---|---|---|---|---|
| | | 3 ft. | 4 ft. | 5 ft. | 6 ft. | 8 ft. |
| 0° | 0° | 24 db | 31 db | 29 db | 29 db | 29 db |
| 0° | 90° | 25 db | 24 db | 27 db | 26 db | 25 db |
| 90° | 0° | *27 db | *26 db | *28 db | *24 db | *20 db |
| 90° | 90° | 26 db | 27 db | 28 db | 29 db | 25 db |
| 45° | 45° | 29 db | 22 db | 24 db | 23 db | *25 db |
| 45° | 135° | 29 db | 31 db | 31 db | 32 db | 27 db |
| 135° | 45° | 26 db | 21 db | 21 db | 21 db | 22 db |
| 135° | 135° | *22 db | *21 db | *24 db | *24 db | *21 db |

*Measurements performed at 123Mc using NASA battery operated signal generator.

Table 2

400Mc Chamber Reflectivity Levels

| Track Orientation $\theta_T$ | Dipole Orientation $\theta_D$ | Dipole Heights Above Floor | | | | |
|---|---|---|---|---|---|---|
| | | 2 ft. | 4 ft. | 5 ft. | 6 ft. | 8 ft. |
| 0° | 0° | 31 db | 39 db | 31 db | 35 db | 32 db |
| 0° | 90° | 39 db | 39 db | 31 db | 32 db | 31 db |
| 90° | 0° | 31 db | 32 db | 32 db | 31 db | 30 db |
| 90° | 90° | 31 db | 32 db | 32 db | 32 db | 31 db |
| 45° | 45° | 31 db | 39 db | 39 db | 34 db | 32 db |
| 45° | 135° | 32 db | 31 db | 30 db | 31 db | 32 db |
| 135° | 45° | 35 db | 32 db | 31 db | 35 db | 30 db |
| 135° | 135° | 32 db | 32 db | 30 db | 31 db | 39 db |

Data taken at 1,200Mc are not presented because later tests prove that the radome is the major contributor to standing waves within the chamber and therefore does not truly represent the capability of a vertical test range.

To verify the fact that the radome was the major contributor to the problem (i.e., larger reflection coefficients than anticipated and polarization sensitivity) measurements were performed with the source antenna inside the chamber just under the radome and compared to the pattern taken through the radome (Figure 13(a)). Thus, an interference pattern (see Figure 13(b)) between incident and reflected energy was produced by essentially removing the radome from between the source and receive antenna. In both cases a horn antenna was moved across the chamber at a 45° angle (from the vertical). The +45° refers to the horn antenna being tilted toward the chamber wall containing the wall mount. And -45° refers to an angle toward the wall without the wall mount.

Plots in Figure 14 compare the standing waves of the A-sandwich radome for the two polarization conditions E-perpendicular and E-parallel as defined below.

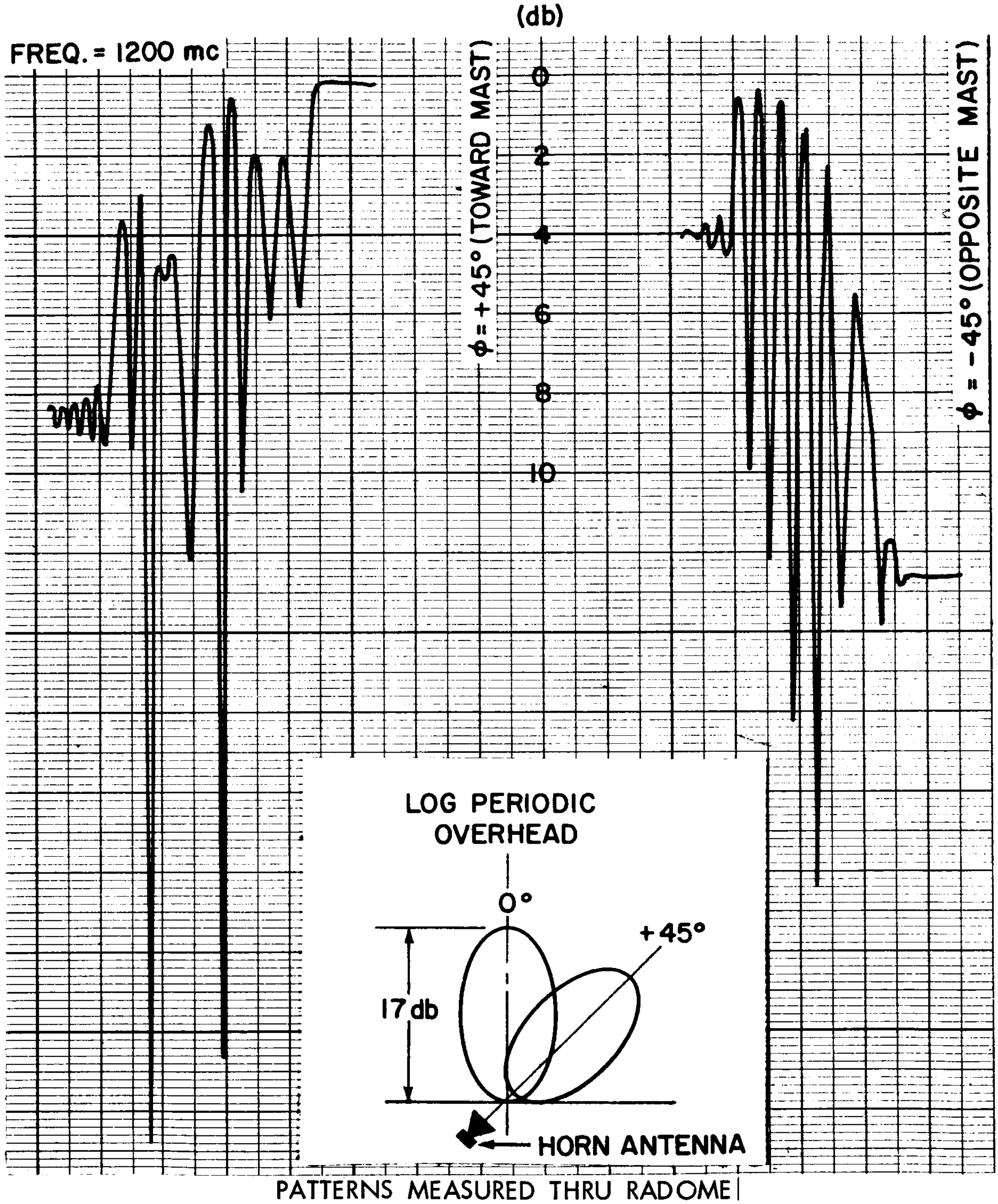


Figure 13a–Radiation Plots Showing Effect of Radome on Reflection Coefficient at 1200 Mc

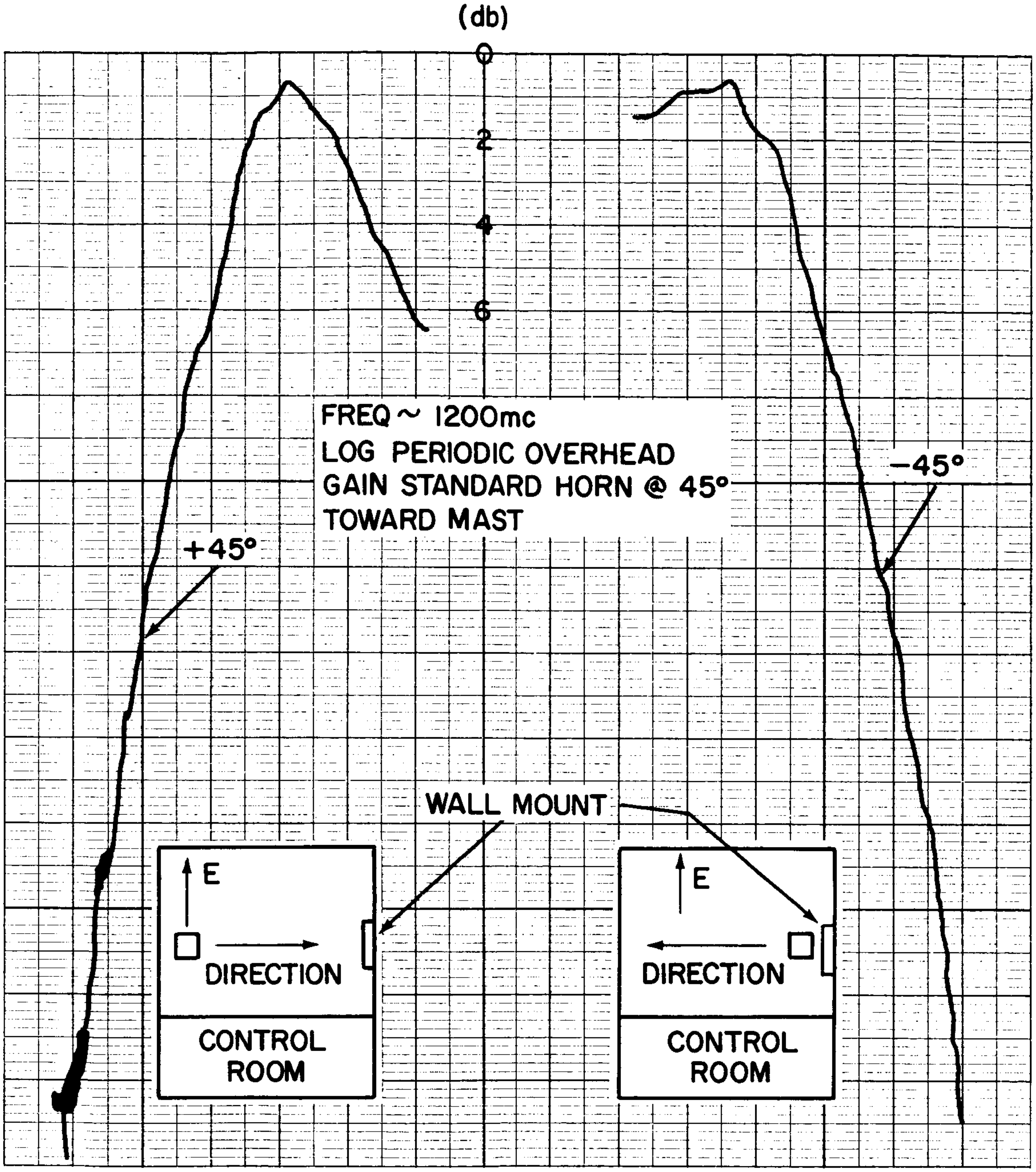


PATTERNS MEASURED UNDER RADOME

Figure 13b–Radiation Plots Showing Effect of Radome on Reflection Coefficient at 1200Mc

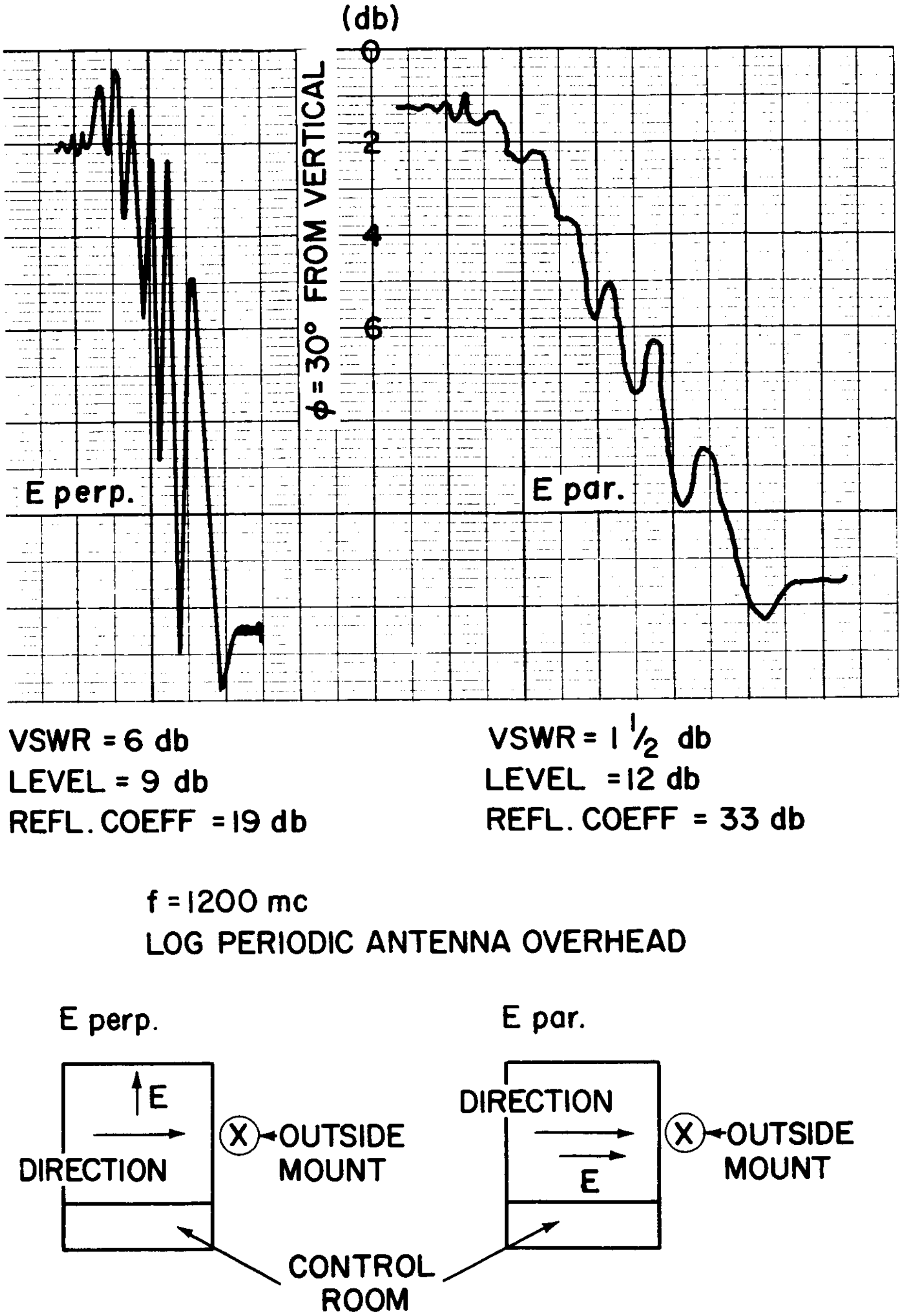


Figure 14–Effect of Radome on Parallel and Perpendicular Polarization

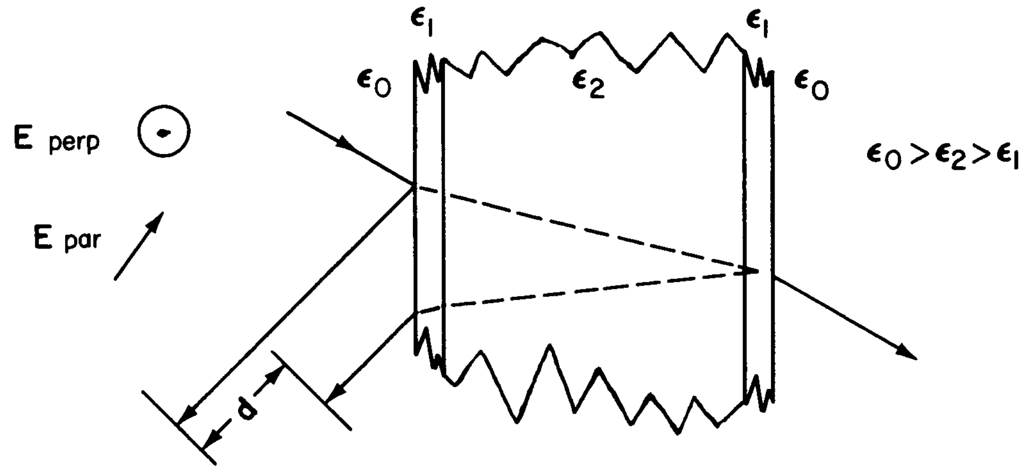


Except at angles far off normal incidence reflected energy from E-perpendicular is nearly always greater than from E-parallel because of the zero at the Brewster angle occurring only with parallel polarization. From Figure 14 it can be seen that the difference in reflection coefficients is 14 db. The Brewster angle (where the reflection value goes to zero) is defined as follows:

$$\theta_B = \tan^{-1}\sqrt{\frac{\epsilon_2}{\epsilon_1}} \quad \text{where } \epsilon_2 > \epsilon_1$$

An important point which is illustrated in Figure 15(a), (b) is the degree of accuracy with which the antenna radiation petterns can be measured through a radome which exhibits significant reflection characteristics. In this case the radiation patterns of an antenna (gain standard at 1,200Mc) was measured first in a free space pattern range method and then the measurement was repeated inside the vertical chamber. To measure the pattern

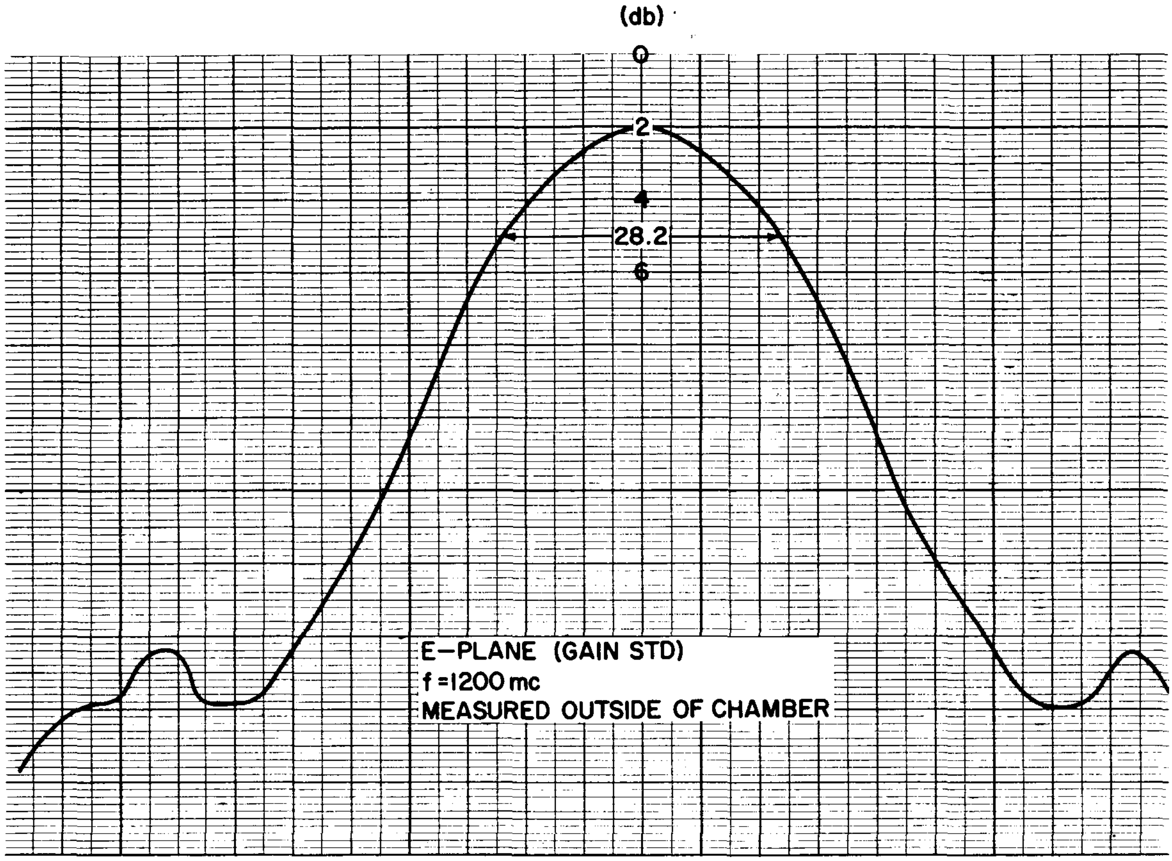


Figure 15a–Pattern of Horn Antenna (E-plane) Measured Outside and Inside of Chamber

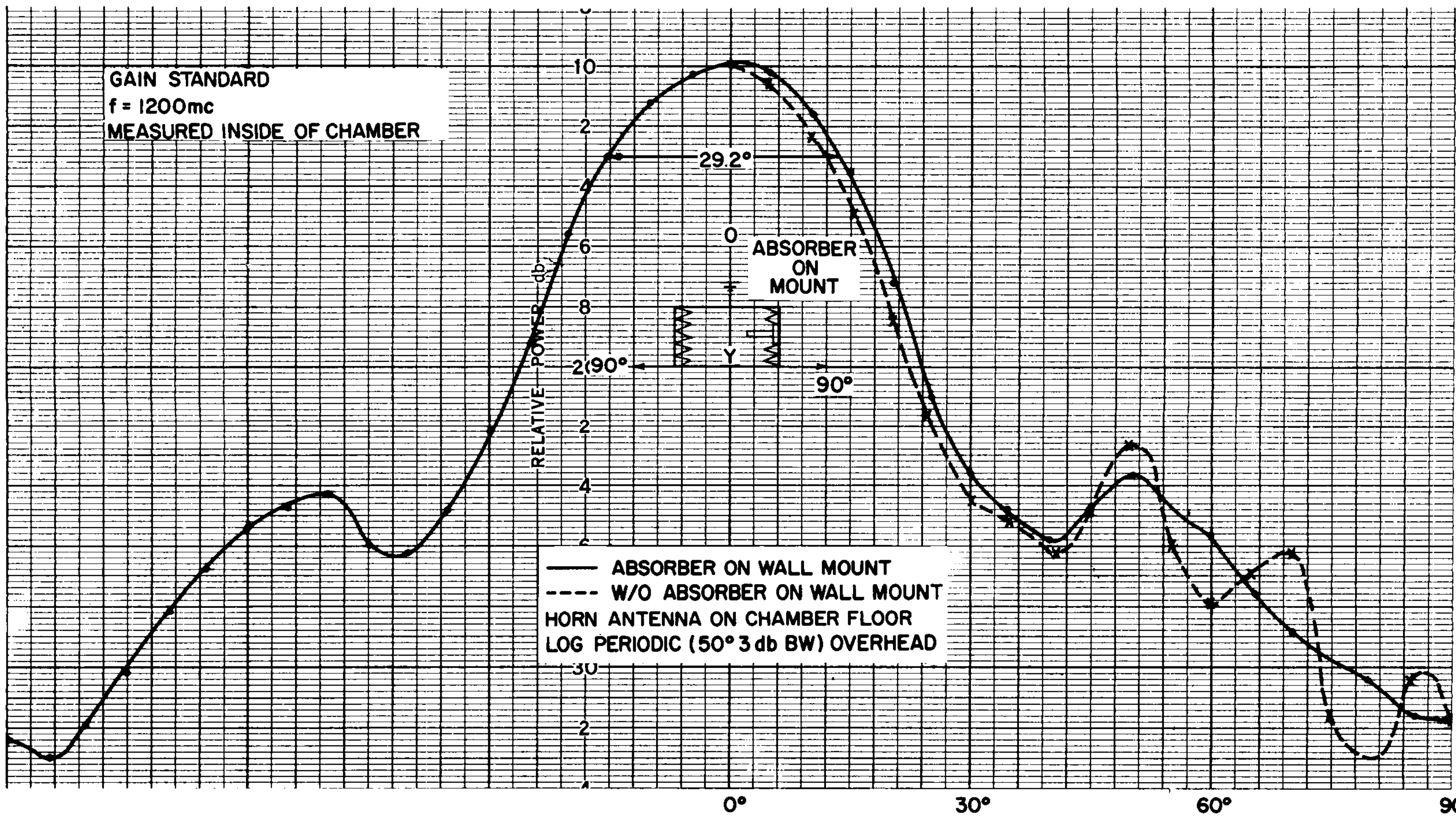


Figure 15b–Pattern of Horn Antenna (E-Plane) Measured Outside and Inside of Chamber

inside the chamber, the antenna was rotated about a fixed axis and not moved across the chamber. Therefore, the "available" reflections which exist across the chamber are not probed and therefore, a rather respectable pattern can be achieved. As a matter of interest Figure 15(b) shows the effect the wall mount can produce in terms of reflected energy.

## IV. CONCLUSIONS

Measurements taken from the 1/9th-scale model of the test range are in reasonable agreement with the measurements of the full scale range. The structural A-sandwich radome definitely reduces the performance of the facility at higher frequencies, but does not affect operation in the frequency range of primary interest (125—400Mc).

The concept of a vertical test range composed of an electrically small termination chamber with a r-f transparent radome has been found feasible and provides at moderate cost a convenient, quasi-all-weather, facility for accurate measurement of antenna characteristics.

## V. RECOMMENDATIONS

Considerable confidence may be placed on the results of measuring scale models of anechoic chambers. Since the instrumentation is not difficult and the cost is small it is recommended that more extensive use be made of scale models to check chamber and anechoic material performance.

A multipanel sandwich radome has definite frequency limitations when used as part of an antenna test range. Therefore it is recommended that a thick, low-dielectric-constant foam radome be used.

## REFERENCES


1. Buckley, E. F., "Outline of Evaluation Procedures for Microwave Anechoic Chamber", Microwave Journal, August, 1963.

2. Emerson, W., "Chamber Information", unpublished report of B. F. Goodrich Company.

3. Jasik, "Antenna Engineering Handbook", New York: McGraw-Hill Book Company, 1961.

4. Harvey, "Microwave Engineering", New York, Academic Press, 1963.

5. Electronic Space Structures Corporation, "Ground Radomes", 1964.